UCRL-16460

University of California

Ernest O. Lawrence Radiation Laboratory

THE PROTON SYNCHROTRON AS A RADIATION SOURCE

Berkeley, California

DISCLAIMER

UCRL-16460

UNIVERSITY OF CALIFORNIA

Lawrence Radiation Laboratory
Berkeley, California

AEC Contract No. W-7405-eng-48

THE PROTON SYNCHROTRON AS A RADIATION SOURCE

Ralph H. Thomas

January 25, 1965

1. Introduction

Weak focussing proton synchrotrons which are currently in operation lie in the energy range 1 to 12.5 GeV.[1, 2] To date, only three strong focussing proton machines have been built, but these have proved so successful in operation[3, 4, 5] that several others are either under construction or planned.. Although the highest energy at present achieved is 33 GeV, (AGS-Brookhaven), it is clear that strong focussing, alternating gradient machines are capable of energies up to several hundred, if not a thousand, GeV. A machine in the U.S.S.R. at Serpukhov designed for an energy of 70 GeV is expected to be in operation in 1966[6], whilst machines of 60,[7] 200[8] and 300 GeV[9] are actively under consideration by groups at Saclay, Berkeley and CERN respectively. The committee under the chairmanship of N. F. Ramsey[10] further recommended that a machine of between 600 and 1000 GeV[11] should be built in the United States in the early 1980's after the successful operation of a 200 GeV machine. Preliminary design studies for 500 GeV and 1000 GeV machines are underway in the Soviet Union[12, 13]. Proton intensities of $\sim 10^{12}$ protons per pulse have been achieved with these machines and it is not unreasonable to expect improvements up to $\sim 10^{14}$ protons pulse. Tables II and III in Section 2.2.2.1[2] list the characteristics of proton synchrotrons at present operating. It should be kept in mind that constant improvement is being made and that intensity figures tend to change rapidly.

Because of the great success of strong focussing machines, their economy and the good optical properties of their proton beams, the weak focussing proton synchrotron is probably obsolescent. At energies greater than about 1 GeV the A.G. synchrotron becomes the prime contender. For this reason, much more attention will be given here to strong focussing machines although, of course, in many respects, as sources of radiation both types of synchrotron are very similar.

It is not our purpose here to give a detailed description of the design features, construction or operation of proton synchrotrons which has been done with great competence elsewhere.[14, 15] For completeness, a brief description of these machines is given in Section 2.2.2.1[16] (see Section A).

Whenever, either by accident or design, the proton beam strikes material, a nuclear cascade is generated. A study of the mechanisms causing beam loss and the ensuing nuclear cascade is of vital importance

in understanding the sources of radiation from synchrotrons which are of two distinct types--the radiation produced when the machine is in operation and the radioactivity induced in the structure of the machine itself, which produces a continued hazard after the machine is turned off.

2. Beam Loss Mechanisms

Generally speaking, beam loss from the injector presents no problem (except close to the electrostatic inflectors). This is because the beam loss is small and the injection energy is relatively low. For many machines it is possible to work in the close proximity of the operating injector (e.g., Brookhaven AGS, Bevatron). However, new machines with higher intensities will demand higher injection energies (e.g., 200 MeV is proposed as the injection energy into the 8 GeV re-injector for the 200 GeV PS). In these cases it may be necessary to provide some shielding at the high energy end of the injector or have a rather elaborate safety system to protect personnel working close to the injector.

We consider in some detail the following causes of beam loss:

(a) Loss at injection
(b) Gas scattering
(c) Loss at transition
(d) Losses at full energy due to targetting and extraction
(e) Operational and accidental losses

(a) Beam Loss at Injection

The choice of injection energy is a compromise between the conflicting demands of cost, beam intensity, residual and stray magnetic fields, gas scattering, etc. At Birmingham[1] it is as low as 460 keV and an electrostatic generator is used, whilst at CERN[1] it is 50 MeV and a linear accelerator is used. Future machines will have linac injection at energies of 200 MeV or higher.[8, 9] Beam is steered into the main ring vacuum chamber by an inflector system. With the linac injection into synchrotrons, it is present practice to "dump" the unwanted linac beam pulses in the neighborhood of the inflector plates. (For example, the Brookhaven AGS linac has a repetition rate of 2.5 pulses per sec.--with the main ring operating at 1 pulse in 2.4 sec., with only 1 linac pulse in 6 being used.) This "beam dumping" has two deleterious effects--high neutron levels are produced whilst the machine is operating and the residual radioactivity after turn-off is often considerable.. Measurements of the radiation levels on top of the Brookhaven AGS shield above the inflector are more than double the average levels nearby.[17] About 6 m from the inflector the dose rate a few hours from shut down after operation at 3×10^{11} protons per pulse is in excess of 100 mr hr^{-1}. Measurements at CERN with somewhat higher beam intensities show levels as high as 2 R hr^{-1} close to the inflector vacuum pipe even

24 hours after shutdown.[19] Dose rates much higher become impractible for normal work within the machine building and so it will be necessary in future machines to avoid beam dumping in the inflector system. The simplest solution would be to "turn off" the injector when not required, but linear accelerators in particular do not work well under these conditions. An alternative solution is to guide the injector beam into a well-shielded dump between synchrotron pulses. The problems of radioactivity induced in the machine proper may then be minimized and the beam dump adequately designed to handle materials of high specific activity.

Present injection techniques at the CERN-PS and Brookhaven AGS have been described by Livingston and Blewett.[14] As the beam enters the main ring vacuum chamber, it very rapidly loses its r-f structure so that when the main ring r-f system is switched on the circulating beam roughly forms a d-c filament. Adiabatic turn-on of the r-f can, in principle, trap all the beam into phase-stable buckets. In practice, with the existing rate of r-f turn-on between 60 and 75% of the beam is trapped. Particles not trapped are lost to the walls but the time taken to lose the untrapped beam can be rather large. Measurements by Distenfeld indicate that loss after injection occurs for several millisecs.[20] The explanation for this rather long loss time is probably a rather complicated combination of the effects of changing magnetic field, radio-frequency and the phase oscillations which have a frequency of ~ 8 kcs for the AGS[21] compared with the circulation frequency of ~ 500 kcs.

(b) Gas Scattering Losses

Losses due to gas scattering fall naturally into three categories:

(i) Multiple coulomb scattering when the beam fills the aperture of the machine.

(ii) Multiple coulomb scattering when the beam is being accelerated.

(iii) Nuclear and diffraction scattering throughout the machine cycle.

In a well-designed proton synchrotron, the injected beam almost entirely fills the available aperture of the vacuum tank. The first weak focussing and strong focussing synchrotrons to be constructed had very large vacuum chambers because the beam orbit stability was not well understood. However, the second generation machines constructed and at present being designed do not have excessive aperture simply for reasons of economy.

Generally speaking, gas scattering losses are not serious. Measurements of the Cosmotron beam life-time[22] indicates $\tau \sim$ 20 secs at a pressure of 2×10^{-6} mm Hg. At 30 GeV, Cumming[23] estimates the AGS beam loss at ~ 0.2% at 2×10^{-6} mm Hg, whilst estimates of beam life-time in storage rings proposed for the CERN-PS are ~ 33 hours at a pressure of 10^{-8} mm Hg.[24] Care must be taken, however, to ensure that the vacuum system is adequate and estimates of beam loss in each individual case are necessary. Extended injection times, for example, when the beam almost completely fills the available aperture can result in significant loss.

(i) Multiple Coulomb Scattering The combined effects of many small angle coulomb scatters and betatron oscillations can produce beam loss, particularly when the beam fills the available aperture. The theoretical treatment of multiple-coulomb scattering losses are contained in papers by Blachman and Courant,[25] Greenberg and berlin,[26] and Courant.[27]

For small loss the probability of survival, P, for a coasting beam occupying some factor a_o of the aperture a may be shown to be:

$$P = 1 - b\sqrt{\eta} \tag{1}$$

where b is a constant to be evaluated in each particular case (see eqn.4) and η is given by:

$$\eta = \frac{2\pi N Z^2 e^4 c R^2}{a^2 \nu^2 E^2 \beta^3} \log \frac{183}{Z^{1/3}} \tag{2}$$

with N = number of residual gas nuclei cm^{-3}.

Z = atomic number of residual gas.

e = electronic charge.

c = velocity of light.

R = radius of beam orbit.

a = semi-aperture of vacuum chamber.

ν = number of betatron oscillations per revolution.

E = total energy of proton.

β = velocity of protons in units of c.

For nitrogen this becomes:

$$\eta = 9.26 \times 10^4 \frac{p R^2 t}{a^2 \nu^2 \beta^3 E^2} \tag{3}$$

when p is measured in mm Hg.

E is in MeV.

Thus the beam loss is directly proportional to $\sqrt{p}$ and $\sqrt{t}$ but inversely proportional to a and E, the total energy of the proton. The value of the constant α in equation (1) may be evaluated from the equation:

$$P(p,t) = \frac{4 \sum_{1}^{\infty} J_1 \{\lambda_s \frac{a_o}{a}\} e^{-\lambda_s \eta}}{(\lambda_s \frac{a_o}{a}) \lambda_s J_1(\lambda_s)} \qquad (4)$$

where $P(p,t)$ = probability of beam survival at pressure p in time t,

$\frac{a_o}{a}$ = fraction of aperture occupied by beam,

J_o, J_1 are the usual Bessel functions,

λ_s is the sth . root of J_o.

Two limiting cases are of interest: with beam filling the aperture ($\frac{a_o}{a} \to 1$) and with the beam very small with respect to the aperture ($\frac{a_o}{a} \to 0$). In these situations equation (4) has the following limiting values:

Beam filling aperture: $\frac{a_o}{a} \to 1$ $\qquad P(p,t) \to 4 \sum_{1}^{\infty} \frac{1}{\lambda_s^2} e^{-\lambda_s \eta}$ $\qquad (5)$

Small Beam: $\frac{a_o}{a} \to 0$ $\qquad P(p,t) \to 2 \sum_{1}^{\infty} \frac{1}{\lambda_s} e^{-\lambda_s \eta}$ $\qquad (6)$

Thus by comparing either equation (5) or (6) with equation (1) the constant c may be evaluated. Garren and Lamb[28] have calculated the probability of beam survival in an accelerator with the following parameters:

Maximum energy	200 GeV
Injection energy	6 GeV
Mean radius	7.25×10^4 cm
Betatron oscillations per turn	18.75
Vertical aperture in vacuum chamber	1.73 cm
p = vacuum pressure	3×10^{-7} mm Hg
t	1/3 seconds

They obtain:

$P(p,t) \approx 0.93$ for beam filling the aperture.

$P(p,t) \approx 0.995$ for beam initially occupying a small fraction of the aperture.

Green and Courant[29] have evaluated the beam losses due to multiple scattering during the acceleration cycle. The probability of beam survival $P(\eta)$ is now given by:

$$P(\eta) = 1 - \sqrt{\frac{2\pi}{\eta}}\, e^{-\frac{1}{2\eta}} \qquad (7)$$

where η is now given by:

$$\eta = \frac{7.1\, \pi^2 p\, R_o^3 S^2 Z^2 e^4 \cdot 10^{16}}{4\nu^2 a^2 T_i eV} \left[2 \log \frac{5.3\, a\, \nu\, 10^{-9}}{1.2 \sqrt{S}\, R_o\, \bar{\lambda}\, Z^{1/3} \sqrt{1+3.33\left(\frac{Z}{137\beta}\right)^2}} - 1\right] \qquad (8)$$

where p is the pressure in mm Hg,

R_o = magnetic radius,

S = straight section factor, $1 + \frac{NL}{2\pi R_o}$ where N is the number and L the length of the straight sections,

T_i = kinetic energy at injection,

eV = energy gain per turn,

$\bar{\lambda} = \bar{n}/p$,

β in the logarithmic term is evaluated at $2\, T_i$.

With the parameters previously given and taking eV as 3 MeV per turn, Garren and Lamb[28] estimate:

$$\eta \approx 1.54 \times 10^{-5}$$

showing that, in this particular case, the loss of beam due to multiple coulomb scattering during acceleration is negligible.

(ii) Nuclear and Diffraction Scattering. All the particles which suffer inelastic collisions are lost to the beam. Most of the particles which suffer diffraction scattering are also lost. We show this as follows:

Almost all the diffraction scattering is contained within the first diffraction peak,[30] i.e., within an angle θ such that

$$2\, kr \sin \frac{\theta}{2} = 3.84 \qquad (9)$$

where k = wave number

r = nuclear radius.

In a machine of semi-vertical aperture a, radius R diffraction scattering will produce complete loss if:

$$\theta \gg \frac{a\nu}{R} \tag{10}$$

Or, using Eq. (9) and the fact that $k = \frac{p}{h}$

p = momentum of the proton

h = Plank's constant.

$$p < \frac{3.84\ h}{a\nu\ r_o A^{1/3}} \tag{11}$$

since $r = r_o A^{1/3}$

For the Brookhaven AGS this gives

$$P < 119\ \text{GeV/c}$$

which is certainly true. Hence, typically, diffraction scattering also produces complete loss of beam. The appropriate cross-section which should be used to compute nuclear scattering is then

$$\sigma_{loss} = \sigma_{abs} + \sigma_{diff} = 1.57\ \sigma_{abs} = 71\ A^{2/3}\ \text{mill barns}^{31}. \tag{12}$$

(for nitrogen $\sigma_{loss} = 412$ mb)

The fraction of beam L(p,t) loss is then

$$L(p,t) \approx \frac{2\pi\ R\ n\ \rho\ L}{A} [\sigma_a + K\ \sigma_e] \tag{13}$$

where n = number of turns

ρ = density of gas

L = Avagadro's number

σ_a = total inelastic cross section

σ_e = total elastic cross section

K = a constant between 0 and 1 and depends on the aperture, energy, and value of ν.

In cases where the protons are relativistic, $2\pi\ R\ n \approx tc$ where t is the duration of the acceleration and c is the velocity of light.

Hence

$$L(p,t) \approx \frac{tc\,\rho\,L\,\sigma}{A} \qquad (14)$$

or

$$L(p) \approx 8.42 \times 10^{2} p \text{ protons sec}^{-1} \text{ (with p in mm Hg)}$$

Thus at a pressure of 2×10^{-6} mm Hg and t = 1 sec:

$$L(p) \approx 0.16\%.$$

Clearly then, nuclear interactions produce a very small beam loss.

(c) Transition Losses

In strong focussing machines, the amplitude of radial excursions increases at the transition energy.[32] This beam "blow-up" can lead to beam loss particularly if there are obstructions in the aperture. Measurements of slow neutrons around the AGS by Distenfeld[20] indicate that at transition, under certain conditions, the beam loss increases by about a factor of 3. By careful control of the relative phase of the radiofrequency power, however, it is possible to avoid any significant beam loss at transition. The situation on the CERN PS is very similar.

(d) Loss at Full Energy

At present several techniques of beam production are used on proton synchrotrons:

(i) Internal Targetting (Thick targets) Two types of internal targets are used and may be roughly designated "thick" and "thin" respectively. "Thick targets" are of the order of one nuclear mean free path thick in the direction of the incident proton beam. When placed in the circulating beam a considerable proportion of the protons interact (typically 50%). Those which do not interact lose considerable energy and undergo multiple coulomb scattering. As a consequence after passing through such a target the residual beam is then rapidly lost to the vacuum chamber walls. Betatron oscillations are induced by the target and at positions of maximum amplitude or regions of small aperture inside the vacuum chamber beam is lost. In weak focussing accelerators where the betatron wavelength is longer than the machine perimeter the loss tends to be more uniformly dispersed than with strong-focussing machines where it is located close to the target areas because of the high ν-value of the machines.

Thick targets tend to be used when a secondary beam of particles is required for a relatively short time, e.g. 2 millisecs as in Bubble Chamber experiments. This technique is used on both weak and strong focussing proton synchrotrons.

(ii) Internal Targetting (Thin targets) For many experimental uses thick targets are unsuitable; for example, in the case of many counter experiments the instantaneous counting rates are often too high. By steering the beam slowly on to a thin target (~ one tenth of a nuclear mean free path thick) in the form of a rod only a small fraction of the beam interacts with the target at each traversal. Disturbances introduced in the beam are small, and so multiple traversals of the target may be made, effectively lengthening the duration of the secondary beam. Thin targets are used on both weak and strong focussing machines.

(iii) Fast Extraction on Strong Focussing Machines Recently the CERN-PS has succeeded in extracting almost all of its circulating beam (~ 95%).[33] This is done within one turn of the machine and so is termed "fast." Of the 5% of beam loss about ~ 4.5% will be scraped off within $\lambda/4$ of the septum magnets of the extraction system and the remaining 0.5% will be uniformly lost. It seems likely that extraction efficiencies of ~ 99% will be achieved in the future.

(iv) Energy-Loss Target Method of Extraction On weak focussing machines beam is extracted by means of an energy-loss target and pulsed (or plunged) bending magnets. This system, first proposed by Piccioni et al,[34] utilises the energy loss in a thin target to displace the circulating proton beam so that it passes through a sufficiently high auxiliary magnetic field to deflect the beam out of the vacuum chamber. A subsequent improvement in the technique was suggested by Bennet and Burren[35] who proposed the use of two internal deflecting magnets. Such a system in operation on the Bevatron has been described by Wenzel.[36] About 60% of the circulating beam of the Bevatron may be extracted, the remainder being lost to the walls of the vacuum chamber. Because beam meets obstructions in three different positions within the vacuum chamber and the betatron wavelength is longer than the circumference of the machine, beam is lost fairly uniformly around the chamber (with local maxima close to the energy loss targets and deflecting magnets).

(v) Slow Extraction on Strong Focussing Magnets Slow extraction schemes which remove the circulating in 10^3 to 10^4 revolutions (3-30 millisecs) are now in operation. A non-linear magnetic pertubation is used to drive particles

into resonance, the large amplitude particles being removed first, the small amplitude particles removed later. Measurements by Bovet et al[37] at CERN indicated extraction efficiencies of 50% with a spill time of ~ 100 millisec. Efficiencies of 80% are confidently expected after some modification of the septum magnet. It is not impossible that improvements in technique will eventually enable extraction of ~ 90% of the beam. As with fast extraction, the septum magnet acts as an internal target and ~ 90% of the remaining beam is lost to the walls within ~ $\lambda/4$, the rest being lost around the ring.

(e) Operational and Accidental Losses

Here one must make an intelligent guess as to the magnitude of beam loss. Several causes of beam loss may be imagined.

(i) Machine tune-up
(ii) Magnet and r-f faults
(iii) Accelerator development

At 30 pulses per minute, there are 4×10^4 pulses per day. Thus, only 40 full energy beam pulses going astray could give a loss comparable with nuclear gas scattering. It does not seem reasonable to suppose that tune-up could be carried out in less than about 15 minutes per day or ~ 1% of the running time. Accelerator development would probably occupy about 10% of all running time. If 10% of this time resulted in large beam loss, we again have an average loss of ~ 1%.

(f) Significance of Beam Loss

The higher the energy at which beam is lost from the accelerator, the more serious the consequences both in terms of radiation background when the machine is operating and of the residual radioactivity of the machine components. At very low energies (typically below 50 MeV) protons are very rapidly stopped by ionization, and very few make nuclear interactions. As the energy increases, the ratio of ionization range to nuclear mean path increases rapidly and is unity at about 500 MeV. A larger proportion of protons make nuclear interaction and the number of nucleons produced at each collision increases. Above 1 GeV the number of pions produced begins to become significant. Thus initially one might expect the induced activity in large masses of material per incident proton to increase rather faster than linearly with energy. Above a few hundred MeV, however, the induced radioactivity will increase roughly linearly with energy. A crude measure of the relative importance of

beam loss may be obtained from the concept of a "damage factor" defined as the product of beam loss and average energy at which it is lost. Table I summarizes the beam losses we might expect from a machine such as the Brookhaven AGS with the damage factor estimated relative to unity for internal targetting.

TABLE I

Typical Idealized Beam Losses from BNL AGS

Source of Beam Loss	Fraction of Circulating Beam Lost	Average Energy of Loss	Relative Damage Factor
Injection	0.5	50 MeV	0.001
Gas Scattering	0.002	15 GeV	0.001
Transition	0.006	10 GeV	0.002
Accidents	0.01	15 GeV	0.005
Internal Targets	1.0	30 GeV	1.0
Fast Extraction	0.01	30 GeV	0.01
Slow Extraction	0.1	30 GeV	0.1

The most important source of activity is seen to be due to internal targetting. This result has led to the suggestion that in machines operating at higher intensities, the use of internal targets may have to be limited[38] so that the average damage factor due to internal target use is about equal to that due to extracted beam use. This implies using the internal targets for something like 10% of the running time at full intensity, or its equivalent.

Measurements of the residual radioactivity around the CERN and Brookhaven machines tend to confirm these conclusions. In 1961 Baarli reported measurements of the dose rates measured a few hours after shut down around the PS. Local variations due to the mode of operation were detectable, but a general pattern could be seen. The highest dose rates measured at that time were ~ 4.5 R hr^{-1} 10 cm from the vacuum chamber, close to a target. Around the ring fluctuations in the dose rate are clearly visible with levels varying between a few mr hr^{-1} to nearly 100 mr hr^{-1}. At 1 m from the PS ring the general radiation levels were below 2.5 mr hr^{-1} with the level near a target increasing to 40 mr hr^{-1}. With higher beam intensities levels have increased somewhat over these figures.

At Brookhaven the situation is very similar. At beam intensities of about 2×10^{11} protons pulse^{-1} Distenfeld[39] has made an elaborate series of measurements of the radiation levels about two feet from the vacuum chamber and close to the tunnel walls. Radiation levels range from about 0.25 mr hr^{-1} to several R hr^{-1}. Gilbert[40] has reported a set of measurements of the radiation levels over a matrix of points on a tranverse section of the machine room. It was found possible to explain the measured radiation levels in terms of high levels of specific activity close to the vacuum chamber, the self shielding of the magnet yoke and thermal neutron activation of the tunnel walls. The transverse section used by Gilbert was mid-magnet, and his results show very clearly the self shielding of the magnet yoke. A crude description of the radiation field is then a lobe of radiation emerging from the open side of the C magnet with a fairly constant radiation field above, below and behind the magnet. This constant radiation level is largely due to the residual radioactivity of the tunnel walls.

3. The Nuclear Cascade

Protons are lost from the vacuum chamber, but as soon as they enter matter a cascade is generated. Generally speaking this cascade is produced in the magnet yoke or copper coils of the guide-field magnets or focussing elements around the machine. Only a small fraction of primary particles can escape the vacuum chamber and magnets without undergoing a nuclear interaction. As a consequence, the nuclear cascade is well developed close to the machine itself rendering the components radioactive. The products from these processes then cross the air gap between the machine proper and close-by shielding in a continuation of the nuclear cascade. Our present knowledge of the details of this cascade is somewhat scanty and drawn from many sources - cosmic rays, shielding measurements around existing accelerators, Monte-Carlo calculations of the intra nuclear cascade and numerical solutions of the cascade diffusion equations.

Perkins [41] has summarised the cosmic ray data which leads one to expect no large changes in attenuation length at higher energies. Measurements of the attenuation length of air for shower producing particles are effectively constant in the range from a few GaV up to as high as $\sim 10^7$ GeV. Measurements of the interaction length of high energy particles in nuclear emulsion and 100 GeV[42,43] and 250 GeV[44] give results in fair agreement with the value of 38 cm. found at energies in the range 6-30 GeV[45,50]. Thus no large changes are to be expected in the nuclear interaction cross sections for pions and protons up to at least several hundred GeV.

At energies below 30 GeV, several measurements of attenuation length have been made for neutrons, pions and protons. Basically, all these experiments place a detector at different depths in the shielding material being investigated. The response of the detector depends upon the size of the initial beam and the energy and spatial resolution of the detector. Conditions vary in the different experiments from well collimated and parallel to very wide beams. Detectors used have varied from nuclear emulsions to large Bismuth fission chambers which have a threshold energy response of 50 MeV. A great deal of confusion exists in the literature over the precise use of various terms, and so we define our use of them here. Suppose the following experiment to be carried out: nuclear emulsions are placed at different depths in effectively infinite slabs of material into which is directed a high energy proton beam whose size is small compared to the detectors. (Fig. 1) The emulsions are subsequently scanned for high energy

nuclear interactions - this enables a rough energy cut off to be made by selecting those stars with a required number of high energy products. Emulsions positioned away from the beam axis enable the total number of particles crossing an infinite plane normal to the incident beam direction to be estimated. Figure 2 shows typical results that might be expected from such an experiment. If the "peak" nuclear interaction intensity is plotted, an exponential attenuation length very nearly $\approx \frac{1}{N \sigma_{int}}$ where σ_{int} is the interaction cross section and N the number of nuclei per cm^3. (σ_{int} is of course obtained precisely if we restrict measurements to the primary particles in the beam direction). The plot of nuclear interactions integrated over an infinite plane, however, takes on a rather different form. The curve immediately rises- the number of high energy particles first increases - reaches its maximum "build up" and then decreases the so-called transition region. We define the "Build up Factor" to be that maximum factor by which the integrated intensity is increased over the incident intensity. This subsequent decrease is never strictly exponential, but it is often sufficiently accurate to approximate the total number of high energy particles in the cascade at large depths ($(x/\lambda) \geq 5$) by :

$$I(x) \approx S(E,E_d) I_o e^{-x/\lambda'}$$

where S(E,Ed) is the SOURCE ENHANCEMENT FACTOR and is a function of the incident proton energy E and the energy sensitivity of the detector E_d.

The SOURCE ENHANCEMENT FACTOR S(E,Ed) may be roughly related to the Build up Factor by the following crude argument:-

The maximum in the integrated intensity curve occurs at a depth of approximately $3\lambda'$. At this point the integrated intensity is approximately half that predicted by the exponential. Here:-

$$B(E) \approx 0.5\ S(E) e^{-3}$$

or $$S(E) \approx 10\ B(E).$$

λ' is the effective attenuation length. In general $\lambda' > \lambda$ but at great depths $\lambda' \rightarrow \lambda$.

Most of the measurements made in practice give results somewhere between these two extremes. The larger the size of the detector in comparison with the incident beam, the more nearly will the results approximate to a curve of type B. If the detector used measures only very low energy particles (neutrons of about 5 MeV for example) it is also possible to measure a build up of particles along the beam axis since there are no low energy neutrons in the incident beam.

Patterson[51] has reported measurements of the attenuation of 90, 270 MeV and 4.5 GeV neutrons in light concrete. These measurements were made using ion chambers, a Bi-fission chamber and C2 nuclear emulsions, good agreement being obtained between the different detectors. Throughout this series of measurements, the incident beams used were rather wide. The value of λ_{atten} measured at 270 MeV of 152 gm cm^{-2} may be compared with the Monte Carlo calculation at 300 MeV by Tsao et al[52] of 145 ± 10 gm cm^{-2}.

Lindenbaum[53] describes measurements of attenuation measurements of a 3 GeV proton beam in heavy concrete (ρ = 4.0 - 4.3 gm cm^{-3}), at depths between 3 feet and 13.5 feet. The incident beam was contained within a proton and pion flux ($E_p > 50$ MeV, $E_\pi > 25$ MeV) were measured as a function of depth and distance from the beam axis. After transition, the primary component, ionization density and health dose rate were all attenuated exponentially with mean free path of 130 ± $\frac{16}{9}$ gm cm^{-2} at ~ 1.5 GeV, and 169± 32 gm cm^{-2} at ~ 2.5 GeV.

A series of measurements of the attenuation of 4.5, 6, and 9 GeV pions in steel and ordinary concrete (ρ - 2.3 gm cm^{-2}) has been made by Tinlot et at[54] using counters. These measurements give values of λ_{atten} independent of energy having an average 123 gm cm^{-2} for concrete and 163 gm cm^{-2} for steel. Errors in these measurements are hard to assess, particularly in the case of steel due to the thin shield used (only 2 feet at 9 GeV).

The most extensive experimental studies of the nuclear cascade have been carried out using the CERN-PS by groups from CERN, Hamburg and Hannover, Harwell, Oak Ridge and Stanford. Citron et al[55] used nuclear emulsions to study the attenuation of nuclear active particles in a concrete and earth assembly, with a 24 GeV/c proton beam. More elaborate experiments were later carried out at 9 GeV/c and 20 GeV/c in concrete, and the information obtained from these experiments has been summarized by Thomas.[56] Measurements in the beam direction indicated an attenuation length for nuclear active particles of about 130 gm cm^{-2} at 20 GeV/c and 160 gm cm^{-2} at 9 GeV/c. Determination of fraction of stars produced by neutral particles shows an initial rise in the neutron density levelling off at depths greater than a meter to a fairly constant value (up to depths of 5 m).

An intensive shielding study has recently been made at CERN in steel at 10 and 20 GeV/c. The incident beam was well collimated and 1 cm wide. Measurements of the attenuation and lateral dimensions of the cascade were made using G5 nuclear emulsions, ionization chambers and C^{12} activation detectors. Bindewald et al[57] have reported the experiments in some detail. Measurements of the dose rate indicate an initial build up in the first 80 gm cm^{-2} and subsequent exponential attenuation with slope of 155 gm cm^{-2}.

Very similar results are obtained with the $C^{12}\binom{n,\ 2n}{p,\ np}C^{11}$ detectors which have a threshold at ~ 20 MeV. In both cases, the source enhancement factor appears to be roughly proportional to energy. Measurements of the minimum ionizing particle track density were made with nuclear emulsions. The track density in the beam direction is attenuated with mfp of 120 gm cm^{-2}, whilst the track density integrated over a plane normal to the beam direction shows the typical transition curve and ultimate attenuation length of 165 gm cm^{-2}.

The most recent series of shielding experiments has been carried out at 7 BeV/c in concrete using the Bevatron.[58] Emphasis was placed on the use of activation detectors in these measurements, although G5 and C2 nuclear emulsions were also exposed. Many different detectors were irradiated, including

$$(Al^{27},\ Na^{24})\quad (Ti^{47},\ Sc^{44})\quad (S^{32},\ P^{32})\quad (Mg^{24},\ Na^{24})$$
$$(I^{127},\ I^{126})\quad (C^{12},\ C^{11})\quad (C^{12},\ Be^{7})^{*}$$

Ther is some small variation in the attenuation lengths measured by these various techniques, but it is difficult to decide the errors of these measurements. Largely speaking, λ_{atten} lies within 120 ± 10 gm cm^{-2} for all these detectors.[58] Measurements of the P^{32} β-activity induced in sulphur gave λ_{atten} = 123 gm cm^{-2} in the beam line, with a value closer to 150 gm cm^{-2} for the intensity integrated over a plane.[59] It is , of course, difficult to interpret the exact significance of measurements made using activation detectors. For example, if the C^{11} activity (20 min half-life) produced in C^{12} irradiated in the shield is measured, we have several production mechanisms:

$$\begin{aligned} &C^{12}\ (n,\ 2n)\ C^{11} \\ &C^{12}\ (p,\ 2p)\ C^{11} \\ &C^{12}\ (\pi^{\pm},\ \pi^{\pm}n)\ C^{11} \end{aligned} \qquad (16)$$

The activity measured A is then given by:

$$A \propto \sum_{i=1}^{n} \int_{E_i}^{E_{max}} \varphi_i\ (E)\ \sigma_i\ (E)\ dE \qquad (17)$$

---

*Because of many possible modes of production, only the initial and final isotope is given.

TABLE II

Summary of Attenuation Length Measurements

	Incident Particle	Beam Energy	Shield Material	Density gm cm^{-3}	Detector	λ_{atten} gm cm^{-2}	Ref.	Remarks
UCRL	n	90MeV	Concrete	2.3	BF	81	51	
UCRL	n	270MeV	Concrete	2.3	BF	152	51	
PRINCETON	n	300MeV	Concrete	3.85	MC	145 ± 10	52	
BNL	p	1.5GeV	Concrete	4.0-4.3	CT	130^{+16}_{-9}	53	
BNL	p	2.5GeV	Concrete	4.0-4.3	CT	169 ± 32	53	
UCRI	n	4.5GeV	Concrete	2.3	BF	172	51	
BNL	π	4.5BeV	Concrete	2.3	CT	118 ± 8*	54	*DeStaebler's estimate of error
BNL	π	4.5GeV	Steel	7.8	CT	155 ± 11*	54	*DeStaebler's estimate of error
BNL	π	6GeV	Concrete	2.3	CT	121 ± 8*	54	*DeStaebler's estimate of error
BNL	π	6GeV	Steel	7.8	CT	155 ± 11*	54	*DeStaebler's estimate of error
UCRL	p	6.2GeV	Concrete	2.4	C^{11}	108 ± 20	58	Thomas's estimate of error
UCRL	p	6.2GeV	Concrete	2.4	Al^{27}	112 ± 20	58	Thomas's estimate of error
UCRL	p	6.2GeV	Concrete	2.4	Au^{198}	116 ± 20	58	Thomas's estimate of error
R.L.	p	6.2GeV	Concrete	2.4	S^{32}	123 ± 10	59	
UCRL	p	6.2GeV	Concrete	2.4	G 5	160 ± 20		Unpublished data
BNL	π	9GeV	Concrete	2.3	CT	129 ± 9*	54	*DeStaebler's estimate of error
BNL	π	9GeV	Steel	7.8	CT	179 ± 12*	54	*DeStaebler's estimate of error
RL, ORNL	p	10GeV	Concrete	3.65	G5	164 ± 20	56	
RL, ORNL	p	10GeV	Steel	7.8	G5	119 ± 10	57	
CERN	p	10GeV	Steel	7.8	C^{11}	145 ± 15	57	
CERN	p	10GeV	Steel	7.8	IC	155 ± 16	57	
DESY, SLAC, CERN, etc.	p	20GeV	Concrete	3.65	G5	132 ± 5	56	Weighted mean of results from DESY, CERN, RL, STANFORD
DESY, CERN, SLAC	p	20GeV	Steel	7.8	G5	137 ± 10	57	
CERN	p	20GeV	Steel	7.8	C^{11}	170 ± 17	57	Thomas's estimate of error
CERN	p	20GeV	Steel	7.8	IC	155 ± 16	57	

see over

TABLE II (continued 2)

Summary of Attenuation Length Measurements

Incident Particle	Beam Energy	Shield Material	Shield Density gm cm^{-3}	Detector	λ_{atten} gm cm^{-2}	Ref.	Remarks
p	24GeV	H. and L. Concrete and Earth	2.4, 3.65, 1.5	G 5	145 ± 10	54	

KEY:

BF = Bismuth Fission Chamber

MC = Monte Carlo Calculation

CT = Counter Telescope

C^{11}, S^{32}, Al^{27} = Activation detectors

G5 = Nuclear emulsion

1 C = Ionisation chamber

where there are n production mechanisms by particles of type i,

$\varphi_i(E)$ is the number of particles of type i between E and E + dE,

$\sigma_i(E)$ is the cross-section for production of the required activity by a particle of type i,

E_i is the threshold for this reaction.

However, the fact that the value of λ_{atten} is found to be roughly constant (after transition) when measured with a variety of activation detectors implies an energy spectrum changing only slowly with depth into the shield. This concept of a fairly constant energy spectrum, for all strongly interacting particles, is supported by the calculations of Alsmiller et al. Using a straight-ahead approximation, a set of coupled integro-differential transport equations which describe the nuclear meson cascade is set up. A program has been written to solve these equations numerically, but there is a great dearth of reliable input information. Some experimental and theoretical work is at present underway at Oak Ridge to improve the situation.[60] By introducing several ad hoc assumptions, Alsmiller et al were able to carry a series of calculations of interest in the design of the shield for the Stanford 45 GeV electron accelerator.[61] The computer program has been used to calculate the dose deposition as a function of depth in concrete from an incident 800 MeV proton beam.[62] Calculations have also been made of the nuclear-cascade induced by 24 GeV protons[63] in heavy concrete - at the present time it is not possible to compare the experimental and theoretical results too readily.

Little information is at present available on the structure of the nuclear cascade normal to the beam direction. Measurements of the beam width in the CERN and Berkeley shielding experiments indicate that the "beam" grows roughly linearly with depth into the shield. Further, the "width" as measured by activation detectors seems little different from that determined by nuclear emulsions (at least after a few mean free paths into the shield). This tends to indicate that the concept of a constant energy spectrum may also apply to situations removed from the beam axis. Further experimental information is needed on this point. Alsmiller has shown how the lateral spread of the cascade may be calculated using a perturbation method. As reliable input data becomes available this calculation may become feasible.

The conclusions from these measurements give support to the technique used by Moyer[64] in estimating shielding for the Bevatron. At large depths in the shield the particles associated with a "primary" proton are estimated. Table III shows the particles Moyer estimates to accompany each surviving 6 GeV primary nucleon in a thick concrete shield. These particle densities may be converted to dose rate and estimates of shield thickness made using an attenuation length of 150 gm cm^{-2}.

TABLE III

Estimated Radiation Accompanying Each Surviving 6 BeV Nucleon

Protons (from cascade and evaporation)	4
Charged pions	3
Muons	0.3
Neutrons (from cascade and evaportation in original star plus equal number from secondary collisions)	7
Slow neutrons	70
Electrons (from π^o decay and Compton scattering of capture gammas and nuclear gammas)	10 (?)
Gammas: Enough to yield ionization dose of 3×10^{-4} mr	

We can write

$$D(x) = S(E) \quad D_o e^{-x/\lambda} \quad \text{for } x/\lambda > \sim 3 \tag{18}$$

where $D(x)$ is the dose at depth x.

D_o is the initial dose at $x = 0$.

$S(E)$ is a source enrichment factor and is a function of energy.

The variation of $S(E)$ with energy is not yet certain and depends to some extent upon the thickness of the shield and particles considered. However, for thick shields $S(E)$ is roughly proportional to energy. Fortunately in estimating shielding, the value of $S(E)$ does not have to be known too well.

The latest theoretical treatment of the nuclear cascade is due to Ranft[65] who has used a Monte Carlo method to calculate the charged particle intensity in steel at depths up to about 3000 gm cm^{-2}. Calculations are made for incident proton energies between 10 and 1000 GeV and quite good agreement with the CERN experimental data is obtained.[57] It is to be hoped

that with the recent successful theoretical calculations and increased experimental data, a more complete understanding of the nuclear cascade is not too far ahead.

4. μ-meson Shielding

For accelerators below about 10 GeV μ-mesons produce few problems. This arises because the shield necessary to reduce radiation levels due to nuclear cascade processes to tolerable levels is in excess of the ionization range of the μ-mesons that could contribute to the radiation problems. The higher the intensity of machines below 10 GeV, the more this is true. Lindenbaum[66] pointed out that the Brookhaven AGS and CERN PS were the first proton accelerators where μ-mesons would dominate some radiation problems.

The major source of μ-mesons is π meson and K meson decay. Essentially all pions and about two thirds of kaons decay into a muon and a neutrino. Once the μ-meson is produced its only really significant mode of losing energy is by ionization as its cross section for nuclear interactions is very small (few μ barns).

We have seen that the intensity of strongly interacting particles in a shield is given by:

$$I(x) = S(E)\, I_o e^{-x/\lambda} \tag{15a}$$

where S(E) varies almost linearly with primary proton energy. The effect of increasing the primary energy from E_1 to E_2 is to demand an increase in shield thickness of

$$\Delta x = \lambda \log \frac{S(E_2)}{S(E_1)} = \lambda \log \frac{E_2}{E_1}. \tag{19}$$

if the same radiation level at the shield surface is to be maintained. In the case of a shield determined by μ-mesons, however, an increase in proton primary energy would demand an increase in shield thickness by the factor $\frac{R(E_2)}{R(E_1)}$ where R(E) is the μ-meson range. This is to a good approximation E_2/E_1. Thus, if we consider as an example primary energies of 100 GeV and 200 GeV, the shield increase required for the strongly interacting particles is only about 12 cm of steel, or 50 cm of concrete. For the μ-meson shield the increase is from 54 meters of iron to 94 meters. Keefe[67] has given an approximate treatment of both the one and three dimensional problem.

Solving first the one dimensional problem of a proton interacting in a target and allowing the mesons to decay in a long drift downstream of the target, he shows the μ-meson spectrum at the end of the drift space is:

$$n_\mu(E,\Delta) \approx \frac{1}{\lambda(1-k)} \int_E^{E_{max}} (\Delta)\; S_m(E', x_o)\; \frac{dE'}{E'^2} \tag{20}$$

where Δ = length of drift space.

$S_m(E',x)$ is the differential energy spectrum of the primary meson at depth x, and x_o is the target thickness.

The primary meson of energy E' is assumed to produce a rectangular μ-decay spectrum between kE' and E'.

E_{max} is the smaller of E /k or E_o the primary energy.

By using the differential spectra proposed by Cocconi et al[68], Keefe derives the number of μ-mesons transmitted by a shield. He shows that the effective attenuation length is about 4500 gm cm^{-2}.(cf 150 gm cm^{-2} for strongly interacting particles), increasing to about 6000 gm cm^{-2} at the highest energies (thick shields).

In his treatment of the three dimensional problem Keefe estimates the spread in "beam size" due to multiple coulomb scattering. Typically the mean square radius due to coulomb scattering is the order of a meter in steel over a large range of shield thicknesses. Thus, although a "back stop" for high energy machines will have to be very long, it does not have to be very wide.

Detailed calculations of this problem now underway for several of the new accelerators proposed should throw much light on this very important topic in the next year or so.

5. "Skyshine"

The term skyshine is something of a misnomer in that it usually describes all the radiation reaching points close to the accelerator, whether unscattered or scattered by the ground, air or neighboring buildings. The term "skyshine" was coined when high neutron backgrounds were observed around cyclotrons with little or no roof shielding. Such background is certainly due to the back-scattering of radiation from the atmosphere--hence, the name "skyshine." However, the effect of ground absorption is important for accelerators where, in most cases, the sources of radiation are close to the ground.

Scattered radiation is of importance around a large accelerator since different safety standards have to be met for radiation workers within the accelerator site, and for the civilian population who may reside close to the perimeter. Those people defined as "radiation workers" which includes all staff concerned with maintenance, operation and use of the accelerator, may receive up to a maximum of 0.1 rem per (40 hour) week, whilst members of the general population may not receive more than 0.01 rem in any one week. Assuming permanent occupancy of sites at the laboratory perimeter, this implies that the average dose rate should be less than 0.06 mr hr^{-1}.

It is of great importance, therefore, to know what radiation levels are produced at the perimeter of the laboratory site by radiation leaking through the shielding, man-holes, equipment access doors, etc. A knowledge of the radiation field around the accelerator will also be helpful in making the decision where to site laboratories and offices close to the machine.

(a) The Propagation of Radiation to Distant Location from a Point Source

In discussing this problem, we assume that the major radiation hazard outside the shielding is due to "fast" neutrons of about 1 - 5 MeV in energy. This is certainly the experience with existing accelerators;[69] the special consideration of muon background is ignored here, it being assumed that specially designed shielding around target areas will eliminate this hazard.

To investigate the nature of the radiation field, we need first to know the variation of neutron flux with distance from a point neutron source. Lindenbaum[70] was the first person to give consideration to this matter. Essentially he used the expression for the neutron flux produced by a point source in an infinite isotropic scattering medium derived by Case et al[51], using diffusion theory. They write the flux $\varphi(r)$ in the form:

$$\frac{4\pi^2\varphi(r)}{Q} = e^{-\Sigma_t(r)}\,\epsilon(c,r) + r\frac{K(c)}{D}\,e^{-k_o r} \qquad (21)$$

with Σ_t = total macroscopic sross-section

D = diffusion coefficient

k_o = diffusion length

$\epsilon(c,r)$ and $K(c)$ are functions of c (ratio of scattering to total cross-sections).

Lindenbaum shows that for 1 - 5 MeV neutrons in air, equation (21) becomes:

$$\varphi(r) = \left[\frac{8.5 \times 10^{-5}}{r^2}\exp(-r/450)\,\epsilon(c,r) + \frac{4.7 \times 10^{-7}}{r}\exp(-r/830)\right]_{r \text{ in feet}} \qquad (22)$$

The importance of the second term is immediately apparent in that it dominates after 100'. The effect of the ground is approximated by taking a value of c of 0.8 to 0.9 (c for air alone is 0.97) based on an albedo for the ground between 0.5 and 0.8. Figure 3 shows curves of $\frac{4\pi r^2\varphi(r)}{Q}$ as a function of r for c = 0.5 and 0.9.

It has been a difficult task to verify these predictions experimentally for a variety of reasons. The available intensity of most machines has limited the range of measurements to about 300 m; in many cases the effects of scattering and the intercalibration of different neutron detectors together with the uncertain effects of a changing neutron spectrum add to the confusion. Nevertheless, several measurements have been made. Cowan and Handloser[72] have reported measurements of the radiation elvels around the Cosmotron at Brookhaven between 250 feet and 1,000 feet with an ionization chamber. Although not specifically stated, it seems likely that the dose rate was almost entirely due to neutrons. Assuming a variation of the form $\varphi(r) = \varphi_o r^{-n}$, they report a value of n = 2.3 ± 0.2.

Dakin[73] has made measurements of neutron fluxes around the Bevatron between 350 feet and 1,650 feet using a BF_3 counter shielded at the back and sides with concrete. By placing concrete in front of the detector, crude estimates were made of the fast neutron energy spectrum. Dakin interprets his results by assuming the neutron spectrum consists of two groups, the first having an average energy between 1.3 and 4 MeV and the second between 100 and 260 MeV. For both groups, the radial variation of neutron flux was very similar and within the experimental accuracy did not differ greatly from inverse square. More recent measurements[74] have been made of the low energy group of neutrons with greater precision. These measurements were made with a moderated BF_3 counter between 300 feet and 1,200 feet from the center of the Bevatron. It is apparent

from this latest group of observations that the neutron flux falls off faster than inverse square and could be better represented by an equation of the form:

$$\varphi(r) = \frac{a}{4\pi r^2} e^{-r/\lambda} \qquad (23)$$

over the range of measurements.

Moyer[75] has explained the surprising fact that the radial dependence of both the high energy and low energy neutrons are almost indistinguishable in the range 100 - 500 meters (as observed by Dakin).

Measurements of the propagation of neutrons in the low energy group have been reported by a group from the Rutherford Laboratory.[76,77] This group was fortunate in that downstream of the neutron source was a flat area completely free of buildings. Neutrons were produced by stopping a 30 MeV proton beam in a thick aluminum target, giving a well-defined "point" source about five feet above the ground. Measurements of the mean neutron energy indicated a value close to 0.75 MeV. Absolute measurements of the neutron flux were made using a calibrated long counter at distances between 100' and 2500' whilst fluxes were measured between 3' and 100 with sulphur capsules and moderated indium foils. It was also possible to make and accurate estimate of the neutron source strength and because of this direct comparison with Lindenbaum's prediction may be made. Measurements made at distances up to 980' indicated that equation (21) predicts fluxes considerably higher than those observed (a factor of three at 1000') and that it was not possible to obtain a good fit to an equation of the form of equation (21). Later measurements by Simpson and Laws[78] at distances out to 2500' even further accentuate the divergence.

Tardy-Joubert and de Kerviler[79] have reported measurements made around "Saturne." Unfortunately, they do not give actual numerical data or errors, but show a smooth curve drawn through their points between 37 m and 700 m from the machine. They claim good agreement between their results and Lindenbaum's equation. However, it is clear that their experimental results do not exhibit the same shape as equation (21) and there are at least 30% discrepencies between the two curves.

(b) Comparison of Existing Experimental Data

It is interesting to compare the existing data. Unfortunately, it is not easy to do this since only in the Rutherford Laboratory has a precise estimate of the source strength been made. The most convenient way to show up differences between data is to plot

$$f(r) = \frac{4\pi r^2 \varphi(r)}{Q} \quad \text{as a function of } r.$$

Such a plot removes the $1/r^2$ dependence and enables one to look at the residual terms. Figure 3 shows such a plot for data taken at Berkeley, Harwell and Saturne.* In the case of the Berkeley data, an arbitrary normalization was chosen so that $\frac{4\pi r^2 \varphi(r)}{Q} = 1.0$ at $r = 280$ m. The source strength taken for the Saclay data was obtained by extrapolating the smooth curve back to $r = 0$.

The main features of the curve are the build-up to a maximum of 1.6 at 110 m with return to 1.0 at 280 m and exponential decrease thereafter with slope 267 m. The experimental results of all three laboratories are seen to be in fair agreement. (Discrepancies ~ 6%). One could wish for more measurements between 300 and 800 meters, but it is fairly clear from the existing data that at distances greater than 100 m, predictions from equation (21) are in error. Figure 3 shows two theoretical curves for $c = 0.5$ (corresponding to completely absorbing earth) and $c = 0.9$ and it can be seen that a good fit may not be obtained to the data using equation (21) merely by choosing the correct value of c, since at large distances the variation of flux with distances is quite different from that observed.

The conclusion from all this is that, whilst more data is desirable, particularly at distances greater than 300 m, it is clear from that data already available that equation (21) does not describe the situation at all well.

A very good empirical fit to the data is given by:

$$f(r) = a(1 - e^{-r/\mu})(e^{-r/\lambda}) \qquad r \geq 50 \text{ meters} \qquad (24)$$

with $a = 2.8$

$\mu = 56$ meters

$\lambda = 267$ meters

Table IV shows the excellent agreement between points taken from the Saclay curve and results calculated from equation (24).

---

* The Saturne data is shown by the solid line on the graph. Experimental points are not available.

TABLE IV

Comparison of Measured and Calculated Values of f(r)

r (meters)	f(r) (measured)	f(r) (calculated from (24))
50	1.30	1.29
75	1.55	1.56
100	1.61	1.60
150	1.56	1.49
200	1.36	1.28
400	0.63	0.62
500	0.42	0.43

A very convenient representation of the variation of neutron flux as a function of distance from a point source is then:

$$\varphi(r) = \frac{Q}{4\pi r^2} \quad f(r) = \frac{aQ}{4\pi r^2} (1-e^{-r/\mu}) e^{-r/\lambda} \qquad (25)$$

for $r \geq 50$ meters.

It is of interest to note that the value of attenuation mean free path for the "skyshine" neutrons obtained from measurements around accelerators is in fair agreement with that found around reactors. Stephens et al[80] using facilities at the Nevada Test Site found $\lambda \approx 245$ yards (224 meters). There are, of course, differences in the neutron spectra in the two cases.

The general shape of the function f(r) shows a build up very similar to that observed in the high energy nuclear cascade (Section 3) and the value of λ (32 gm cm^{-2}) is in fair agreement with that measured for fast neutrons in concrete (~ 29 gm cm^{-2}).

km

ACKNOWLEDGMENTS

It is a pleasure to acknowledge the many colleagues who were kind enough to provide unpublished experimental information. In particular Dr. J. B. Cumming and Mr. C. Distenfeld provided much information concerning the BNL AGS, and the LRL Health Physics Group provided much data on the Bevatron. Dr. D. Keefe made many helpful suggestions as to the form and content of this section.

REFERENCES

[1] Barton, M. Q., "Catalogue of High Energy Accelerators," BNL-683(T-230) 1961.

[2] Madey, R., Tables 2 and 3, "Nuclear Accelerators," Section 2.2.2.1, Engineering Compendium on Radiation Shielding, Vol. 1.

[3] Standley, P. H., "Status Report on the CERN Proton Synchrotron," "Proceedings of the International Conference on High Energy Accelerators," Dubna, August 21-27, 1963, Page 99.

[4] Green, G. K., "AGS Performance and Plans," op.cit., Page 110.

[5] Barabash, L. Z. et al, "Status Report on the 7 GeV ITEP PS," op.cit., Page 137.

[6] Vladimirsky, V. V. et al, "The 60-70 GeV Proton Synchrotron," op.cit., Page 195.

[7] Bronca, G. et al, "The French 60 GeV Project," op.cit., Page 202.

[8] Smith, L., "Berkeley Study for a Proton Synchrotron," op.cit., Page 80.

[9] Johnson, K. et al, "The CERN Design Study for a 300 GeV Proton Synchrotron," op.cit., Page 40.

[10] Ramsey, N. F., "Report of the Panel on High Energy Accelerator Physics of the General Advisory Committee to the Atomic Energy Commission and the President's Science Advisory Committee," TID-18636 (1963).

[11] "Experimental Program Requirements for a 300-1000 BeV Accelerator and Design Study for a 300-1000 BeV Accelerator," BNL 772 (T290) (1963).

[12] Vladimirsky, V. V. et al, "A 500 GeV Proton Synchrotron," Proceedings of the International Conference on High Energy Accelerators. Dubna. August 21-27, 1963, Page 86.

[13] Burshtein et al, "A 1000 GeV Cybernetic Accelerator," op.cit., Page 67.

[14] Livingstone, M. S. and Blewitt, J. P., "Particle Accelerators," McGraw Hill (New York) 1962.

[15] Livingood, J., "Cyclic Particle Accelerators," De Van Nostrand (Princeton) 1961.

[16] Madey, R., "Nucleon Accelerators," Section 2.2.2.1 (This Volume).

[17] "A Proposal for Increasing the Intensity of the Alternating Gradient Synchrotron at the Brookhaven National Laboratory," BNL 7956 (1964) Page 229.

[18] Distenfled, C., (BNL) Private communication.

[19] Baarli, J., (CERN) Private communication.

[20] Distenfeld, C., (BNL) Private communication.

[21] Green, G. K. and Courant, E. D., "The Proton Synchrotron," Handbuch der Physik, Vol. 44., Page 334 (1959). Springer Verlag (Berlin).

[22] Cottingham, J. G., BNL-7534, Page 228 (1963).

[23] Cumming, J. B., "Studies of Radioactivity at High Energies," Proceedings of the 1963 Summer Study on Storage Rings, Accelerators and Experimentation at Super High Energies," BNL-7534, 392 (1963).

[24] Middlekoop, W. C. and deRaad, B., CERN Report AR/Int. SG 64-6 (1964).

[25] Blachmann, N. M. and Courant, E. D., Phys. Rev. 74, 140 (1948)
Phys. Rev. 75, 315 (1949).

[26] Greenburg, J. M. and Berlin, T. H., Rev. Sci. Inst. 22, 293 (1951).

[27] Courant, E. D., Rev. Sci. Inst. 24, 836 (1953).

[28] Garren, A. A. and Lamb, W. A. S., UCID-10016 (1954).

[29] Green, G. K. and Courant, E. D., "The Proton Synchrotron," Handbuch der Physik, Vol. 44, 335 (1959) Springer Verlag (Berlin).

[30] Akheiser, A. and Pomeranchuk, I., J. Phys. U.S.S.T. 9, 471 (1945).

[31] Keefe, D. and Scolnick, M., AS/Experimental/01 (UCLRL internal document), December 10, 1964.

[32] Green, G. K. and Courant, E. D., "The Proton Synchrotron," Handbuch der Physik, 44, 335 (1959) Springer Verlag (Berlin).

[33] Bertello, R. et al, "The Fast Ejection System of the CERN 25 GeV Proton Synchrotron," Proceedings of the International Conference on High Energy Accelerators. Dubna. August 21-27 (1963), Page 669.

[34] Piccioni, O. et al, Rev. Sci. Inst. 26, 232 (1955).

[35] Bennet, R. G. T., and Burren, J. W., J. Nuc. Energy, Part C, 3, 14 (1961).

[36] Wenzel, W. A., "Bevatron External Beam," Proceedings of the International Conference on High Energy Accelerators. Dubna. August 21-27, 1963, Page 698.

[37] Bovet, C., Lambertson, G. H., and Reich, K. H., CERN 64-25 (1964).

[38] "A Proposal for Increasing the Intensity of the Alternating Gradient Synchrotron at the Brookhaven National Laboratory," BNL 7956 (1964), Page 226.

[39] Distenfeld, C., Private communication.

[40] Gilbert, W. S., UCID-10137 (1964).

[41] Perkins, D. H., UCRL-10022 (1961), Page 58.

[42] Barkow, A. G. et al, Phys. Rev. 122, 617 (1961).

[43] Farrow, E. et al, Nuovo Cimento 28, 1238 (1963).

[44] Lohrman, E. et al, Phys. Rev. 122, 672 (1961).

[45] Rajopadhye, V. J., Phil. Mag. 5, 537 (1960).

[46] Winzeler, H. et al, Nuovo Cimento, 17, 8 (1960).

[47] Bogachev, N. P. et al, Dok. Akad. Nauk. USSR 121, 617 (1958).

[48] Bricman, C. et al, Nuovo Cimento 20, 1017 (1961).

[49] Jain, P. L. et al, Nuovo Cimento 21, 859 (1961).

[50] Barbaro-Galtieri, A. et al, Nuovo Cimento 21, 469 (1961).

[51] Patterson, H. W., "First International Conference on Shielding around High Energy Accelerators," Page 95, Paris, 1962.

[52] Tsao, C. J. et al, "Monte Carlo Calculations of the Shielding of the Princeton-Pennsylvania 3 BeV Proton Synchrotron," Preprint (1958).

[53] Lindenbaum, S. J., Ann. Rev. Nuc. Sci. 11, 213 (1961).

[54] Tinlot, H., Private communication.

[55] Citron, A. et al, Nuc. Inst. and Methods 14, 97 (1961).

[56] Thomas, R. H. (editor), NIRL/R/40 (1963).

[57] Bindewald, H. et al, Nuclear Instruments and Methods (to be published).

[58] Smith, A. R., UCRL-11331 (1964).

[59] Shaw, K. B., Private communication.

[60] Alsmiller, R. G., Private communication.

[61] Alsmiller, R. G. et al, ORNL-3289 (1962), ORNL-3365 (1963), ORNL-3412 (1963).

[62] Alsmiller, R. G. and Murphy, J. E., ORNL-3406 (1963).

[63] Alsmiller, R. G. and Murphy, J. E., ORNL-3367 (1963).

[64] Moyer, B. J., TID-7454 (1957), UCRL 9769 (1961).

[65] Ranft, J., CERN 64-47 (1964).

[66] Lindenbaum, S. J., Ann. Rev. Nuc. Sci. 11, 248 (1961).

[67] Keefe, D., UCID-10018 (1964).

[68] Cocconi, G. H. et al, UCRL-10022 p. 167 (1961).

[69] See (for example) Smith, A. R., UCRL-8377 (1958).

[70] Lindenbaum, S. J., TID-7454 p.101 (1957).

[71] Case, K. M. et al, "Introduction to the Theory of Neutron Diffusion," Vol. 1 Los Alamos. (1953).

[72] Cowan, F. P. and Handloser, J. S., BNL-264 (T-43) (1953).

[73] Dakin, H. S., UCID-1281 (1961).

[74] Dakin, H. S., Internal Memo. Health Physics Department LRL, University of California (1962).

[75] Moyer, B. J., "First International Conference on Shielding around High Energy Accelerators," page 65 Paris (1962).

[76] Thomas, R. H., op.cit. page 83.

[77] Thomas, R. H., et al, NIRL/M/30, March 1962.

[78] Simpson, P. W. and Laws, D., Private communication (August 1962).

[79] Tardy-Joubert, P. and deKerviler, H., CEA 2303 (1963).

[80] Stephens, L.D. et al, Lawrence Radiation Laboratory, Private communication.

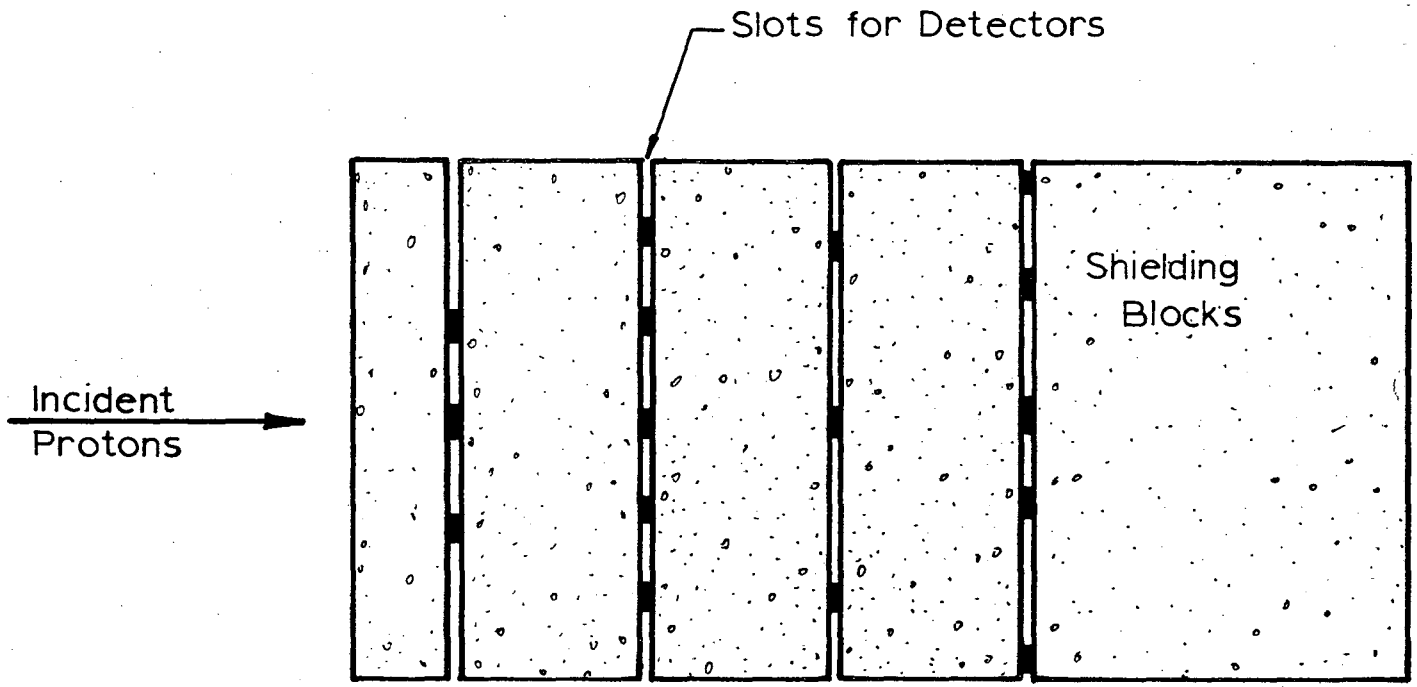

Shielding Experiment Schematic

fig. 1

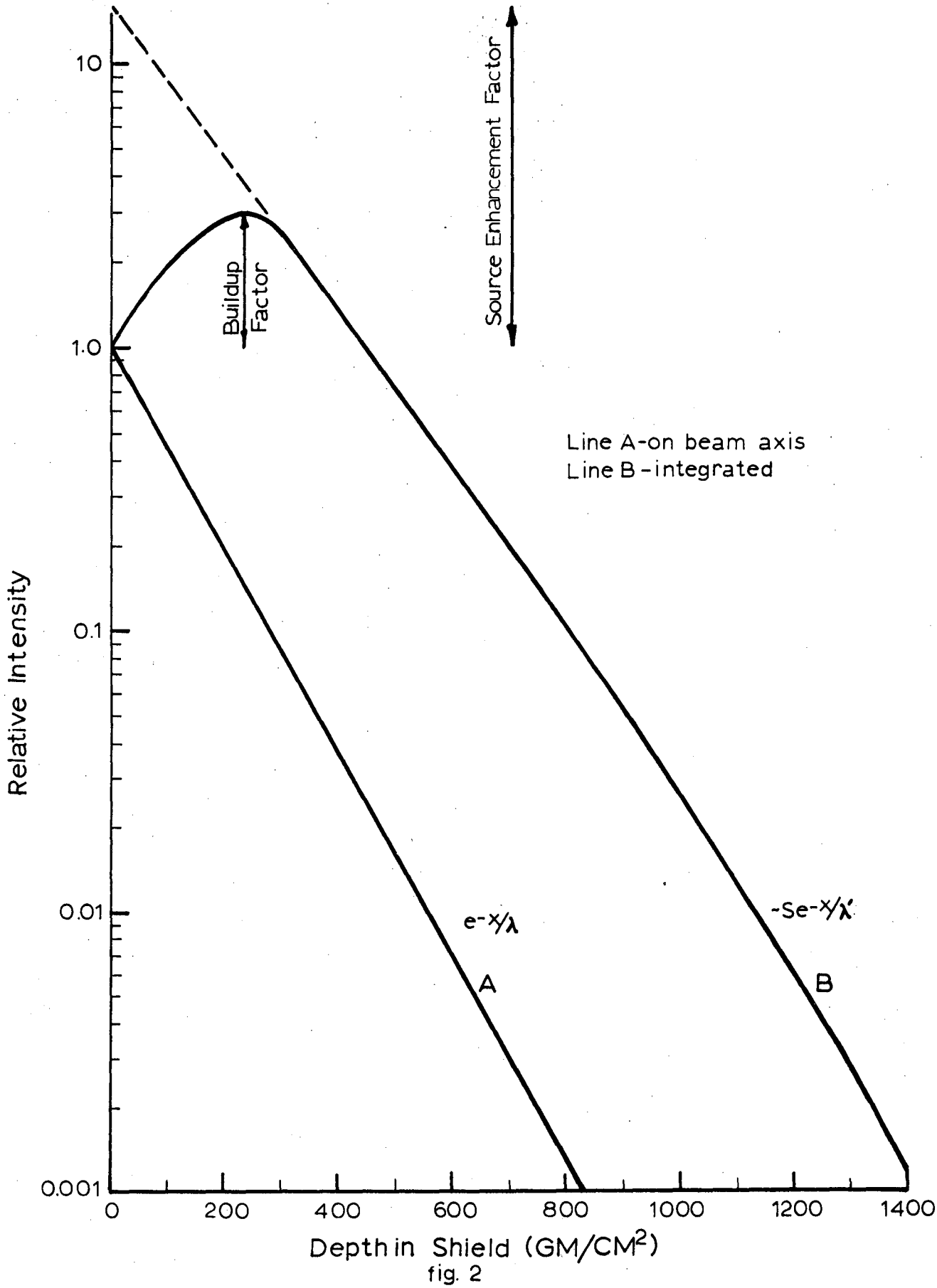
10
1.0
0.1
0.01
0.001
Relative Intensity
Buildup Factor
Source Enhancement Factor
Line A-on beam axis
Line B-integrated
e-x/λ
A
-Se-x/λ'
B
0
200
400
600
800
1000
1200
1400
Depth in Shield (GM/CM2)

fig. 2

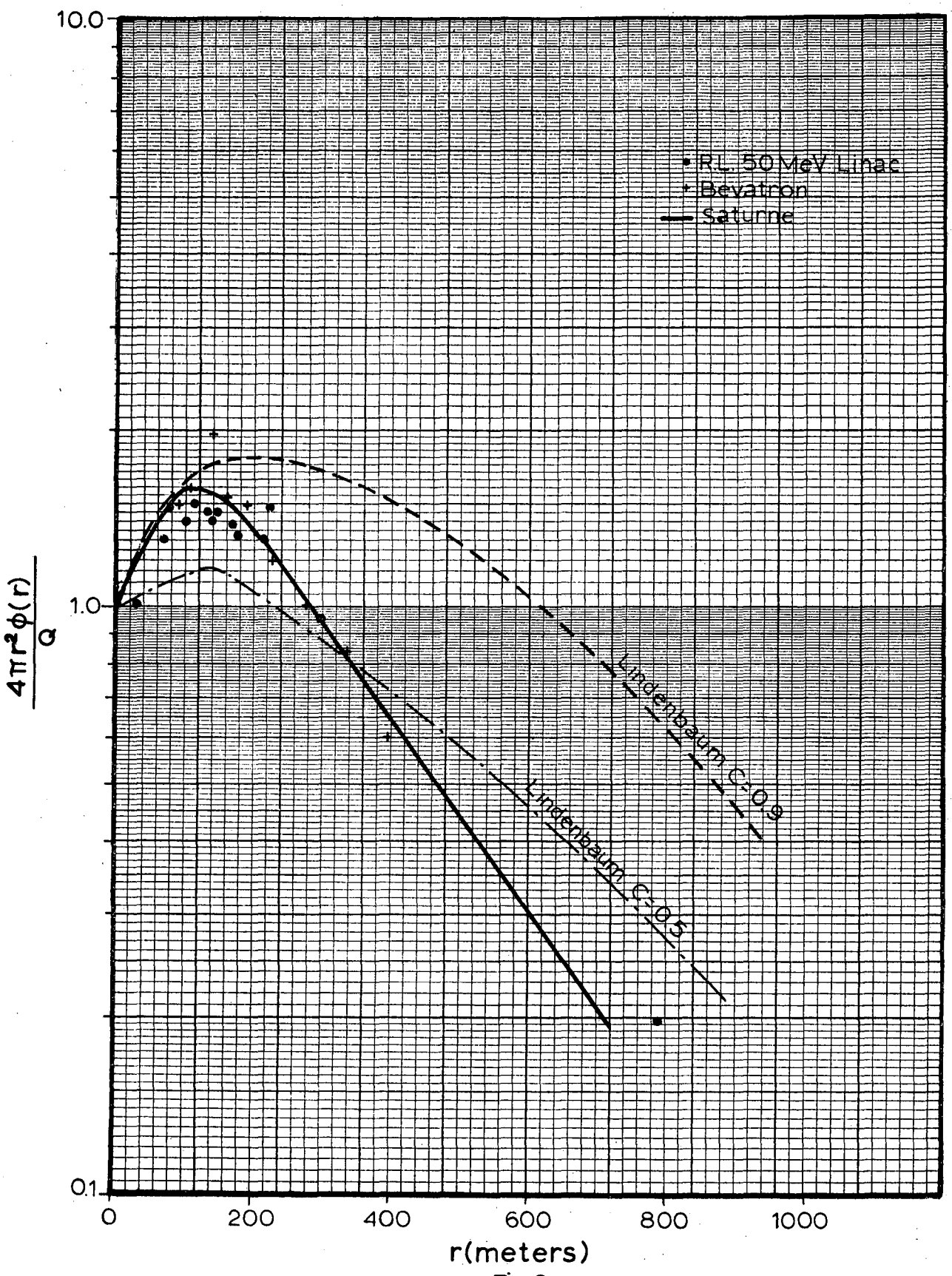
10.0
1.0
0.1
$\frac{4\pi r^2 \phi(r)}{Q}$
0
200
400
600
800
1000
r(meters)
• R.L. 50 MeV Linac
• Bevatron
— Saturne
Lindenbaum C=0.9
Lindenbaum C=0.5

Fig. 3